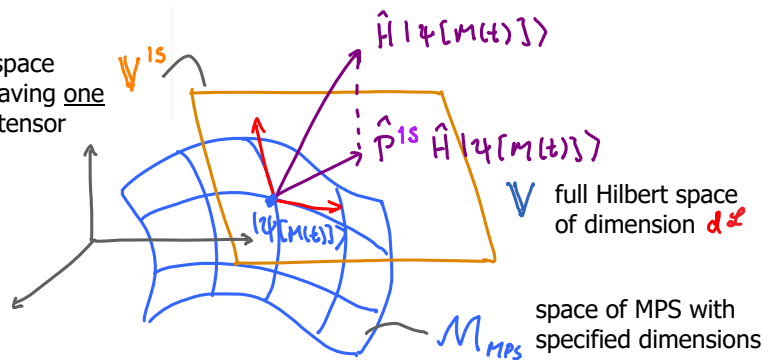


We consider time evolution using 'time-dependent variational principle' (TDVP)

1. 1-site TDVP [Haegeman2016, App. B]

Schrödinger equation for MPS:

$$i \frac{d}{dt} |\Psi[M(t)]\rangle = \hat{H} |\Psi[M(t)]\rangle \quad (1)$$



$$i \frac{d}{dt} \left[\begin{array}{c} A_1 \quad A \quad A_L \quad \Lambda_L \quad B_{L+1} \quad B_L \\ \text{---} \sigma_e \quad \sigma \end{array} \right] \quad (2)$$

if we insist on using MPS with fixed bond dimensions, left side has following form:

$$= \sum_{\ell'=1}^{\ell} \begin{array}{c} \dot{A}_{\ell'} \\ \text{---} \sigma_e \quad \sigma \end{array} + \begin{array}{c} \dot{\Lambda}_{\ell} \\ \text{---} \sigma_e \quad \sigma \end{array} + \sum_{\ell'=L+1}^L \begin{array}{c} \dot{B}_{\ell'} \\ \text{---} \sigma_e \quad \sigma \end{array} \quad (3)$$

Each term differs from $|\Psi(t)\rangle$ by precisely one site tensor or one bond tensor, so left side is a state in the tangent space, V^{1s} of $|\Psi(t)\rangle$. But right side of (1) is not, since $\hat{H} |\Psi(t)\rangle$ can have larger bond dimensions than $|\Psi(t)\rangle$.

So, project right side of (1) to V^{1s} : $i \frac{d}{dt} |\Psi[M(t)]\rangle \simeq \hat{P}^{1s} \hat{H} |\Psi[M(t)]\rangle \quad (4)$
 tangent space approximation

Left and right sides of (4) are structurally consistent. To see this, consider bond ℓ

Left side of (4) contains:

$$\frac{d}{dt} \begin{array}{c} A_{\ell} \quad \Lambda_{\ell} \quad B_{\ell+1} \\ \text{---} \sigma_e \quad \sigma \end{array} = \begin{array}{c} \dot{A}_{\ell} \quad \Lambda_{\ell} \quad B_{\ell+1} \\ \text{---} \sigma_e \quad \sigma \end{array} + \begin{array}{c} A_{\ell} \quad \dot{\Lambda}_{\ell} \quad B_{\ell+1} \\ \text{---} \sigma_e \quad \sigma \end{array} + \begin{array}{c} A_{\ell} \quad \Lambda_{\ell} \quad \dot{B}_{\ell+1} \\ \text{---} \sigma_e \quad \sigma \end{array} \quad (5)$$

Decompose: $\dot{A}_{\ell} \Lambda_{\ell} = A_{\ell} \dot{\Lambda}'_{\ell} + \bar{A}_{\ell} \bar{\Lambda}'_{\ell}$, $\Lambda_{\ell} \dot{B}_{\ell+1} = \Lambda''_{\ell} B_{\ell+1} + \bar{\Lambda}''_{\ell} \bar{B}_{\ell+1} \quad (6)$

Then we find:

$$\frac{d}{dt} \begin{array}{c} A_{\ell} \quad \Lambda_{\ell} \quad B_{\ell+1} \\ \text{---} \sigma_e \quad \sigma \end{array} = \begin{array}{c} \bar{A}_{\ell} \quad \dot{\Lambda}'_{\ell} \quad B_{\ell+1} \\ \text{---} \sigma_e \quad \sigma \end{array} + \begin{array}{c} A_{\ell} \quad \dot{\Lambda}_{\ell} \quad B_{\ell+1} \\ \text{---} \sigma_e \quad \sigma \end{array} + \begin{array}{c} A_{\ell} \quad \bar{\Lambda}''_{\ell} \quad \bar{B}_{\ell+1} \\ \text{---} \sigma_e \quad \sigma \end{array} \quad (7)$$

Right side of (4) requires tangent space projector. Consider its form (TS-I.5.25):

$$P^{1s} = \sum_{\ell'=1}^{\ell'} \begin{array}{c} \text{---} \sigma_e \quad \sigma \end{array} + \sum_{\ell'=L+1}^L \begin{array}{c} \text{---} \sigma_e \quad \sigma \end{array} \quad (8)$$

$$p^{1s} = \sum_{\bar{l}=1}^{l'} \text{diagram} + \text{diagram} + \sum_{\bar{l}=l'+1}^L \text{diagram} \quad (\text{II})$$

The three terms with $\bar{l} = l$, $l' = l$, $\bar{l} = l+1$, applied to $\hat{H} |\Psi(t)\rangle$, yield

$$\text{diagram} + \text{diagram} + \text{diagram} \quad (4)$$

matching structure of (7). Thus, p^{1s} , applied to $H(\Psi(t))$, yields terms of precisely the right structure!

To integrate projected Schrödinger eq. (4), we write tangent space projector in the form (TS.5.26):

$$p^{1s} = \sum_{l=1}^L \text{diagram} - \sum_{l=1}^{L-1} \text{diagram} \quad (10)$$

and write (4) as

$$\left. \begin{aligned} & i \sum_{l=1}^L \text{diagram} \\ & i \sum_{l=1}^{L-1} \text{diagram} \end{aligned} \right\} := \sum_{l=1}^L \text{diagram} - \sum_{l=1}^{L-1} \text{diagram} \quad (11)$$

Right side is sum of terms, each specifying an update of one ψ_l^{1s} or ψ_l^b on the left. Eq. (4) can be integrated one site at a time, by defining the updates through the following local Schrödinger equations:

$$i \dot{c}_l := \text{diagram} H_l^{1s}, \quad i \dot{\lambda}_l := - \text{diagram} H_l^b \quad (12)$$

In site-canonical form, site l involves two terms linear in c_l : $i \dot{c}_l(t) = H_l^{1s} c_l(t)$ (13)

Their contribution can be integrated exactly: replace $c_l(t)$ by $c_l(t+\tau) = e^{-iH_l^{1s}\tau} c_l(t)$ forward time step (14)

In bond-canonical form, site l involves two terms linear in λ_l : $-i \dot{\lambda}_l(t) = H_l^b \lambda_l(t)$ (15)

Their contribution can be integrated exactly: replace $\lambda_l(t)$ by $\lambda_l(t-\tau) = e^{iH_l^b\tau} \lambda_l(t)$ (16)

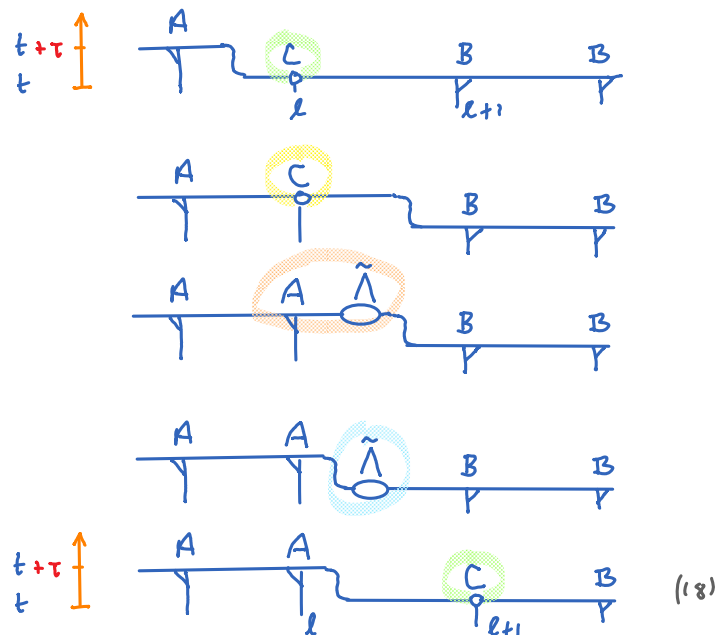
In practice, $e^{-iH_2^{15}\tau} C_f$ and $e^{iH_2^b\tau} \lambda_e$ are computed by using Krylov methods.

Build a Krylov space by applying H_ℓ^{1s} multiple times to C_ℓ , set up the tridiagonal representation $[H_\ell^{1s}]_{\text{Krylov}}$ of H_ℓ^{1s} in this basis, then compute the matrix exponential in this basis, and apply result to C_ℓ . Likewise for H_ℓ^b and Λ_ℓ .

To successively update entire chains, alternate between site- and bond-canonical form, propagating forward or backward in time with H_ℓ^s or H_ℓ^b , respectively:

1. Forward sweep, for $l = 1, \dots, L-1$, starting from $C_l(t) := \downarrow B_1(t) B_2(t) \dots B_l(t)$ (17)

$$\begin{aligned}
 & C_e(t) B_{e+1}(t) \\
 & \xrightarrow[1(b)]{H_L^{15}} C_e(t+\tau) B_{e+1}(t) \\
 & = \underbrace{A_e(t+\tau) \hat{\Lambda}_e(t+\tau)}_{1(b)} B_{e+1}(t) \\
 & \xrightarrow[1(c)]{H_L^b} A_e(t+\tau) \underbrace{\hat{\Lambda}_e(t) B_{e+1}(t)}_{1(d)} \\
 & = A_e(t+\tau) C_{e+1}(t)
 \end{aligned}$$



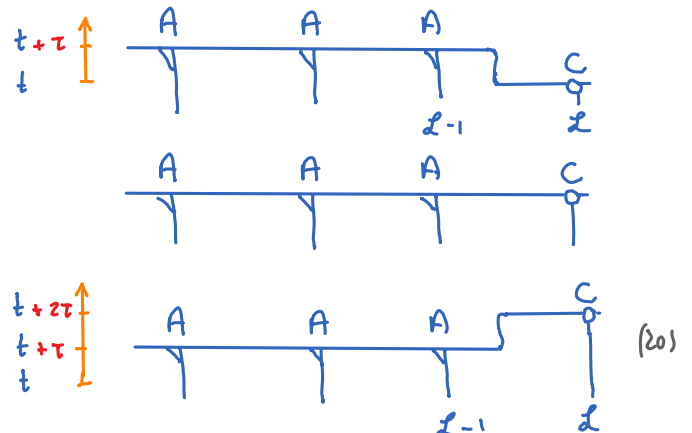
until we reach last site, and MPS described by

$$A_1(t+\tau) \dots A_{L-1}(t+\tau) C_L(t) \quad (19)$$

2. Turn around: $C(t)$

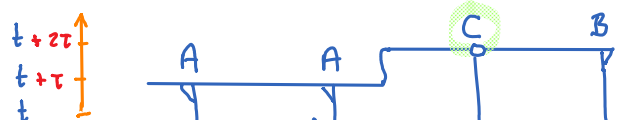
$$\frac{H_x^{15}}{z(a)} \rightarrow C_x(t+\tau)$$

$$\frac{H_x^{15}}{z(b)} \rightarrow C_x(t+2\tau)$$



3. Backward sweep, for $l = L-1, \dots, 1$, starting from $A_l(t+\tau) \dots A_{l-1}(t+\tau) C_L(t+\tau) \quad (2)$

$$A_l(t+\tau)C_{l+1}(t+2\tau)$$



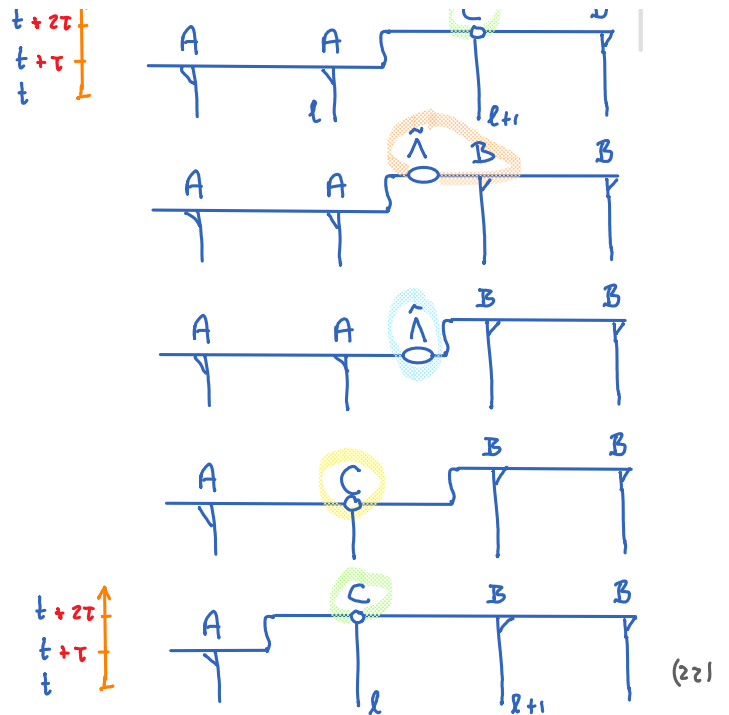
$$A_l(t+\tau) C_{l+1}(t+2\tau)$$

$$\stackrel{3(a)}{=} A_l(t+\tau) \tilde{\Lambda}_l(t+\tau) B_{l+1}(t+2\tau)$$

$$\stackrel{3(b)}{H_l^b} \rightarrow A_l(t+\tau) \tilde{\Lambda}_l(t+\tau) B_{l+1}(t+2\tau)$$

$$= C_l(t+\tau) B_{l+1}(t+2\tau)$$

$$\stackrel{3(d)}{H_l^{is}} \rightarrow C_l(t+2\tau) B_{l+1}(t+2\tau)$$



until we reach first site, and MPS described by $C_1(t+2\tau) B_2(t+2\tau) \dots B_L(t+2\tau)$ (23)

The scheme described above involves 'one-site updates'. This has the (major!) drawback (as in one-site DMRG), that it is not possible to dynamically explore different symmetry sectors. To overcome this drawback, a 'two-site update' version of tangent space methods can be set up [Haegemann2016, App. C].

A systematic comparison of various MPS-based time evolution schemes has been performed in [Paeckel2019]. Conclusion: 2-site-update tangent space scheme is most accurate!

A scheme for doing 1-site TDVP while nevertheless expanding bonds, called 'controlled bond expansion' (CBE), was proposed in [Li2022] (see next lecture!).

We focus on $\eta = \zeta$ (but general case is analogous). Define space of 2-site variations:

$$\mathcal{V}^{2S} = \text{span of all states } |\Psi'\rangle \text{ differing from } |\Psi\rangle \text{ on at most } 2 \text{ neighboring sites}$$

$$= \text{span} \left\{ |\Psi'\rangle = \begin{array}{c} \xrightarrow{\quad} \circ_l \text{---} \overset{\text{2 sites}}{\circ_{l+1}} \xrightarrow{\quad} x, \ell \in [1, L-1] \end{array} \right\} \quad (I)$$

formal definition: $= \text{span} \left\{ \underset{\substack{\uparrow \\ \text{image}}}{\text{im}(P_{\ell}^{Z^s})} \mid \ell \in [1, \ell-1] \right\}$ (2)

local 2s projector:
 $l \in \{1, L-1\}$

$$P_L^{z,s} = \text{Diagram 1} \quad \text{Diagram 2} \quad \text{Diagram 3} \quad (3)$$

Global 2s projector \hat{p}^{2s} , such that $V^{2s} = im(\hat{p}^{2s})$, can be found with a Gram-Schmidt scheme analogous to our construction of \hat{p}^{1s} , see [Gleis2022a]:

compare (TS-I.5.22)

$$p^{2s} := \sum_{\ell=1}^{\ell'-1} \underbrace{p_{\ell}^{2s}}_{p_{\ell}^{2s} - p_{\ell+1}^{1s} = p_{\ell, \ell+1}^{DK}} + p_{\ell'}^{2s} + \sum_{\ell=\ell'+1}^{\ell-1} \underbrace{p_{\ell}^{2s}}_{p_{\ell}^{2s} - p_{\ell}^{1s} = p_{\ell-1, \ell+1}^{KB}} \quad \text{for any } \ell' \in [1, \ell-1] \quad (4)$$

$$p^{2s} = \sum_{l=1}^{l'-1} \left(\text{diagram 1} \right) + \left(\text{diagram 2} \right) + \sum_{e=l'+1}^{\infty} \left(\text{diagram 3} \right)$$

All summands are mutually orthogonal, ensuring that $(p^{zs})^2 = p^{zs}$, and that $p^{zs} p_{\ell'}^{zs} = p_{\ell'}^{zs}$.

Alternative expression:
compare (TS.5.26)

$$P^{2S} = \sum_{l=1}^{L-1} P_l^{2S} - \sum_{l=1}^{L-2} P_{l+1}^{1S} = \sum_{l=1}^{L-1} \left(\text{Diagram 1} \right) - \sum_{l=1}^{L-2} \left(\text{Diagram 2} \right) \quad (7)$$

This projector is used for 2-site TDVP (see TS-II.3)

Orthogonal n-site projectors

For any given MPS $|\Psi[M]\rangle$, full Hilbert space of chain can be decomposed into mutually orthogonal subspaces:

$$V = V_1 \otimes \dots \otimes V_L = \bigoplus_{n=0}^L V^{n\perp} \quad (8)$$

with $V^{0\perp} := V^{0s} := \text{span}\{|\Psi\rangle\}$ (9)

'irreducible' $V^{n\perp}$ is complement of $V^{(n-1)s}$ in $V^{ns} = V^{(n-1)s} \oplus V^{n\perp}$ (10)

= span of states differing from $|\Psi\rangle$ on n contiguous sites, not expressible through subsets of $n' < n$ sites

Correspondingly, identity can be decomposed as:

$$1_V = 1_d^{\otimes L} = \sum_{n=0}^L P^{n\perp} \quad , \quad P^{n\perp} P^{n'\perp} = \delta^{nn'} P^{n\perp} \quad (11)$$

completeness orthogonality

where $P^{\perp n}$ is defined as the projector having $V^{n\perp}$ as image: $\text{im}(P^{n\perp}) = V^{n\perp}$ (12)

$$P^{0\perp} = P^{0s} = |\Psi\rangle\langle\Psi| = \text{diagram with 1 site} \quad (13)$$

$$n \geq 1: P^{n\perp} := P^{ns} (1_V - P^{(n-1)s}) = P^{ns} - P^{(n-1)s} \quad (14)$$

since $V^{(n-1)s} \subset V^{ns} \Rightarrow \text{im}(P^{(n-1)s}) \subset \text{im}(P^{ns})$
 $\Rightarrow P^{ns} P^{(n-1)s} = P^{(n-1)s}$

Consider $n=1$:

$$P^{1\perp} = P^{1s} - P^{0s}$$

(TS-I.5.26)

$$= \sum_{l=1}^{L'} \text{diagram 1} + \text{diagram 2} + \sum_{l=L'+1}^L \text{diagram 3}$$

choose $L' = L$

$$- \text{diagram 4} \quad (15)$$

$$= \sum_{l=1}^L \text{diagram 5} = \sum_{l=1}^L P_{l,l+1}^{2k} \quad (16)$$

projects onto all 1-site variations orthogonal to $|\Psi\rangle$

Consider $n=2$:

(TS.4.17) $P_{l,l+1}^{0s}$

$$P^{2\perp} = P^{2s} - P^{1s} = \left(\sum_{l=1}^{L-1} P_l^{2s} - \sum_{l=2}^{L-1} P_l^{1s} \right) - \left(\sum_{l=1}^L P_l^{1s} - \sum_{l=1}^{L-1} P_l^{0s} \right) \quad (17)$$

$$= \sum_{l=1}^{L-1} (P_l^{2s} - P_{l+1}^{1s} - P_l^{1s} + P_{l+1}^{0s}) \quad (18)$$

move P_L^{1s} from 3rd to 2nd term

$$= \sum_{l=1}^{L-1} \left(\text{diagram 6} - \text{diagram 7} \right)$$

$$- \left(\begin{array}{c} \text{Diagram 1} \\ \text{Diagram 2} \end{array} + \begin{array}{c} \text{Diagram 3} \\ \text{Diagram 4} \end{array} \right) \quad (19)$$

(TS.3.28)

$$= \sum_{l=1}^{L-1} \begin{array}{c} \text{Diagram 1} \\ \text{Diagram 2} \end{array} = \sum_{l=1}^{L-1} P_{l,l+1}^{DD} \quad \text{very important result!} \quad (20)$$

[Haegeman2016, Sec. V & App. C]

2-site tangent space methods are analogous to 1-site methods, but use a 2-site projector. There is a conceptual difference, though: the main reason for using 2-site schemes is that they allow sectors with new quantum numbers to be introduced if the action of H requires this. However, states with different ranges of quantum numbers live in different manifolds, hence this procedure 'cannot easily be captured in a smooth evolution described using a differential equation. However, like most numerical integration schemes, the aforementioned algorithm is intrinsically discrete by choosing a time step, and it poses no problem to formulate an analogous two-site algorithm'. [Haegeman2016, Sec. V]. In other words: the tangent space approach is conceptually not as clean for the 2-site as for the 1-site scheme.

Schrödinger equation, projected onto 2-site tangent space, now takes the form

(1)

$$i \frac{d}{dt} |\psi[m(t)]\rangle = \hat{P}^{2s} \hat{H} |\psi[m(t)]\rangle$$

$$\hat{P}^{2s} = \sum_{l=1}^{L-1} \left(\text{diagram 1} \right) - \sum_{l=2}^{L-1} \left(\text{diagram 2} \right) \quad (2)$$

This yields [compare (1.11)]:

$$\text{or } \left\{ \begin{array}{l} i \sum_{l=1}^{L-1} \text{diagram 3} \\ i \sum_{l=1}^{L-2} \text{diagram 4} \end{array} \right\} := \sum_{l=1}^{L-1} \text{diagram 5} - \sum_{l=1}^{L-2} \text{diagram 6} \quad (3)$$

Right side is sum of terms, each specifying an update of one ψ_e^{2s} or ψ_{e+1}^{1s} on the left. Eq. (4) can be integrated one site at a time, by defining the updates through the following local Schrödinger equations:

$$i \dot{\psi}_e^{2s} := \text{diagram 7} H_e^{2s}, \quad i \dot{\psi}_{e+1}^{1s} := - \text{diagram 8} H_{e+1}^{1s} \quad (4)$$

Right side is sum of terms, each linear in a factor appearing on the left. Can be integrated one site at a time:

$$\text{In 2-site-canonical form, site } l \text{ involves two terms linear in } \psi_l^{2s} : i \dot{\psi}_l^{2s}(t) = H_l^{2s} \psi_l^{2s}(t) \quad (5)$$

$$\text{Their contribution can be integrated exactly: replace } \psi_l^{2s}(t) \text{ by } \psi_l^{2s}(t+\tau) = e^{-i H_l^{2s} \tau} \psi_l^{2s}(t) \quad (6)$$

forward time step

$$\text{In 1-site-canonical form, site } l+1 \text{ involves two terms linear in } \psi_{l+1}^{1s} : -i \dot{\psi}_{l+1}^{1s}(t) = H_{l+1}^{1s} \psi_{l+1}^{1s}(t) \quad (7)$$

Their contribution can be integrated exactly: replace $\psi_{l+1}^{1s}(t)$ by $\psi_{l+1}^{1s}(t-\tau) = e^{iH_{l+1}^{1s}\tau} \psi_{l+1}^{1s}(t)$ (8)
backward(!) time step

To successively update entire chains, alternate between 2-site- and 1-site-canonical form, propagating forward or backward in time with H_l^{2s} or H_l^{1s} , respectively (analogously to 1-site scheme).

A systematic comparison of various MPS-based time evolution schemes has been performed in [Paeckel2019]. Conclusion: 2-site-update tangent space scheme is most accurate!